Experimental and numerical investigation of solar air collector with different porous media obstructions

MSc Shrooq Jomaa Ali[1], Prof. Jalal M. Jalil[2,*], Prof. Assist. Shereen F. Abd Al-Karim[3]
Electromechanical Engineering Department,
University of Technology, Baghdad Iraq

[1]University of Technology, Department of Electromechanical Engineering, Baghdad, Iraq, 50677@student.uotechnology.edu.iq , +9647759623624
[2,*] University of Technology, Department of Electromechanical Engineering, Baghdad, 50003@uotechnology.edu.iq, +9647901339497
[1]University of Technology, Department of Electromechanical Engineering, Baghdad, Iraq, 50041@uotechnology.edu.iq, +9647902176204

Abstract

This work concerns improving thermal efficiency by investigating the experimental and numerical investigation of thermal performance of different types of balls with high and low thermal conductivity (glass and stainless steel balls) as packed beds in the second channel of the collector. The porous media is attached in the lower channel in order to enhance the heat transfer characteristics of the flow. Porosity, solar radiation, mass flow rate and thermal conductivity have been studied. Turbulent flow is implied for continuity, momentum and energy equations of the flow through solar air collectors. Novel CFD application using FORTRAN language was applied, the cells blocked as solid with porosity value. The results show that the thermal efficiency increases with increase in mass flow rate, while the exit temperature decreases for high mass flow rate. The maximum thermal efficiency was achieved with higher thermal conductivity (stainless steel balls) which reached 85.9% at porosity 33.5% while; it reached 76.02% with glass balls at porosity 42.8%. The decrease in porosity increased efficiency. The efficiency with stainless steel balls and glass balls as porous media reached 62 and 45% higher than without porous media.

Keywords: Different Conductivity; Porous Media; CFD; FORTRAN, Double Pass; Solar Collector

1. Introduction

Porous media can be used in different applications to improve heat transfer performance [1-3]. An important application is the solar air heater. Air heater worked by solar energy is a device was used for heating, in effect, work as a device, converting solar flux to heat the air [4]. Air heaters are widely work for drying fruits and vegetables, and crops, food processes, and space heating, as well as low to medium temperature applications [5]. Solar collector construction and maintenance are simple. It doesn't have a fuel cost after setup. Furthermore, avoid corrosion and leakage problems when compared with liquid solar heating system. The air heaters are friendly environmental devices, without CO_2 [6]. The disadvantage of solar heaters are low coefficient of heat of air [7], thus different arrangements for the flow are applied to

enhance thermal performance [8]. Using more than one channel [9] will improve thermal performance of the system. More than one channels were implied specially two passes, in parallel [10], in counter [11] and with recycle [12]. One weak point in those systems is the increase of pressure drop. To enhance the heat transfer [13], a porous media [14], attaching fins [15] and roughness [16] were used. However, each of these steps improves pressure drop and heat transfer in solar air heaters considerably [17].

Alam and Kim [18] reviewed the methods to enhance the thermal performance of two passes collector. Saha [19] analytically investigated the thermal efficiency of the double flow, double and single exposure collectors. Thermal performance was tested by different parameters like mass flow rate and solar irradiation. Results show that solar air collector with double exposure is better than the solar air collector with single exposure. With 0.0277 kg/s of mass flow rate, the two passes collector is 4.17% higher effective than the one pass collector. Meanwhile, Hirasawa et al. [20] used porosity material to decrease heat transfer by natural convection to 7% for absorber temperature 100 °C. Meria et al. [21] reviewed the effect of the porous media on Photo Voltaic thermal system. Dhiman et al. [22] studied the theoretical and experimental investigation of the counter and parallel flow of solar air heaters with using wire mesh as porous media has been dissection. The efficiencies of the double passes in counter fashion with bed packed are (11 – 17 percent) greater than that of double with parallel fashion. In contrast, parallel fashion improved thermal hydraulic performance by 10 percent at differential mass rates compared to the counter flow system. Gupta et al. [23] evaluated output of the two pass solar heater without using permeable medium and also using various types of porous materials such as (steel wool and glass wool) with double pass solar air heaters. Jouybari and Lundström [24] investigated the impact of thin permeable material that has high value of conductivity for the absorber of a collector. Applying a small thickness of porous above an absorber improves performance of the solar air heater. The gain in the performance is much more than that can be gained in a non-permeable material, while the increasing of the factor of the friction of porous collectors is twice that of solar heaters without permeable material. Kareem et al. [25] investigated an improved many-pass solar collector supported by granite pebble bed. Relative humidity and ambient temperature range observed in repeated tests were 48.04–87.9% and 21.09–36.64 °C respectively. System has achieved 72.59 percent maximum thermal collector capacity. The average daily collector efficiency of 36.38% was achieved with 0.016 kg/sec optimum mass flow rate. Singh [26] presented thermal performance investigation with serpentine (porous) wavy at porosity range from 85% to 95% packed bed solar heat numerically and experimentally. The results of the experiments show that the highest thermo hydraulic and thermal efficiencies for porosity equal to 93% serpentine-packed solar air heaters are found approximately 74% and 80% respectively. Numerical results show that maximum thermo hydraulic performance of 24.33% is better for serpentine-packed bed solar air heater compared with flatbed solar air heater. Singh et al. [27] experimentally investigated a two passes converge duct with wire fins system. In addition to the using sixteen numbers of fin in the channel, there are a 10 surfaces of wire mesh like screens with porosity of 96% film in the second channel. The solar air heater's maximum thermo hydraulic and thermal efficiencies are obtained 80% and at 93% at a mass flow rate equal to 0.03 kg/s and 0.023 kg/s respectively. Kansara et al. [28] studied a solar air collector (flat-plate) with fins and porous media. The work have CFD simulation and experiments. Solar simulator was used. The air temperature difference was 16.17% higher than channel without porous. Ahmed and Mohammed [29] studied double pass with porosity

material. The solar collector with porosity material had 2 top and bottom ducts. The fluid flowed in the same direction through the ducts, while the bottom duct was filled with porosity material. Glass balls with a diameter of 15.98 mm and a k value of 0.78 W/m K were used as porous media. The porosity of porous media was 0.437. The porous material collector usually can has high regular efficiency (thermal) of 80 percent, while the other collectors usually can has high efficiency (thermal) of 51 percent. Salah et al. [30, 31] studied a double-pass SAH with paraffin capsules. The period of the discharge and temperature of the air increase were: 3 hours with 3 to 17.95 ^{o}C for 825 W/m^2 at mass flow rate of 0.6 kg/min. Dawood et al. [32] studied the window SAH with 7 perforated absorbent curtains. The proposed window SAH used to heat the coming fluid and balance between solar radiation and heating of the fluid.

Recently, many papers have been published concerning porous media in solar collector. For numerical papers, Fu et al. [33] studied the effect of porous media-assisted in improving thermal efficiency of collector. The improving reached 49%. Siavashi et al. [34] showed that using Nano fluid and porous media increased Nussalt number ten times it is value without porous media. Xia et al. [35] showed that using blocks of metal (porous) improved collector performance by 1.8 times without blocks. Mustafa et al. [36] indicated that using metal foam as porous improved efficiency of the triangular collector and reached 61 to 111%. Helmi et al. [37] showed that enhancing in the energy and exergy reached 80% and from 35%, respectively in collector with trough. Khelifa et al. [38] showed improving in water PVT collector efficiency reaching 70% using porous media (flax-fiber) integrated with the collector. Bozorgi et al. [39] indicated that direct absorption collector efficiency reached 93% by silver water porous wavy. Darbari et al. [40] showed that the efficiency of parabolic trough collector can be improved by disks as porous.

In the study of all the previous literature, few numerical and experimental studies have been found to explore the possibility of different thermal conductivities of porous media. Experimental and numerical investigation of the double pass solar air heater has been studied. Two kinds of permeable materials with different values of conductivities with different porosities have been used. The main objective of this research is studying the effect of thermal conductivity, different mass flow rate, intensity of radiation and type of porous on the thermal efficiency.

2. Equipment's of the Experiments

Figure 1 shows the equipment which are:

1) Collectors of sunlight.
2) Tungsten Halogen lamps.
3) Centrifugal blower.
4) A door for controlling the flow quantity.
5) Temperature sensors.
6) A measurement devices:-
    a) Hot-wire anemometer (Velocity measurement).
    b) Radiation measurement (Solar meter).
    c) Pressure measurement (Digital manometer).
    d) Temperature recorder.

The prototype system has been developed and build. The sun simulator used 8 lamps (halogen) with a 400 W each capacity. Irradiance sets were 300, 400, 500 and 600 W/m^2 at the test surface area measured. Dimmer was used for controlling the amount of solar radiations.

Double pass solar air heaters made from an aluminum collector with dimensions of 1.25 m long, 0.30 m wide, and 0.11 m height. The total height is divided into two parts, the first of which has a 50 mm height and the second of which has a 60 mm height. The absorber plate's length and width are 1.20 m and 0.30 m, respectively, with the length being shorter than the collector's length, so the air flow can go back. Glass with 0.4 cm thickness was used. Insulation has been mounted. For air drawing, the centrifugal blower was used. It is attached to the lower channel's outside in order to move air from the bottom passage. A gate is installed that connects the blower to the bottom passage. The gate is used to regulate the mass of air that flows through it. The position of the porous media is appeared in Figure 2, and the permeable material in aluminum drawer with nets in front of air flow. A wood structure was used to hold the simulator lamps. The solar simulator was equipped with eight halogen lamps (400 W, 220 V). To keep the temperature distribution consistent in the system, the height betwmeen the lamps and the air heater is 0.5 m, and the height between each two halogen lamp is about 0.13 m. The channels of data logger are connected to the thermocouple and distributed throughout the device. Solar power meter used for measuring the irradiation from tungsten lamps into cover glass of the collector. Uncertainty analysis is where the accuracy of model outcomes have been determined.

Two kinds of porous materials (glass and stainless steel balls) will be studied. Glass balls made of strips wrapped and others from stainless glass. It is used for toys and decoration with 0.81 W/m K conductivity at three porosities 57.5, 51.4 and 42.89 percent as shown in Figure 3. The second type of porous media is stainless-steel balls with 20 W/m K conductivity at porosities 62 and 33.5% as shown in Figure 4 which are available in the market.

To make the results more accurate, the uncertainty in the solar collector operation can be estimated using the error rate detected in the instruments used in practical experiments and the following equations.

$$m^{\cdot} = \rho V_{av} A_c \cdots (1) \qquad \text{And}$$

$$\eta = \frac{Q}{I_T A_c} = m^{\cdot} C_p (T_o - T_{in}) / I_T A_c \ldots (2)$$

Where C_P, A_C are assumed to be constant during the experimentation, and the density is a function of pressure and temperature. So, the relation well be come:

$$m^{\cdot} = f(V_{av}, T, P) \cdots (3) \qquad \text{And}$$

$$\eta = f(\dot{m}, T_o, T_{in}, I_T) \cdots (4)$$

$$W_{total} = [(X_1)^2 + (X_2)^2 + (X_3)^2 + \cdots (X_n)^2]^{1/2} \cdots (5)$$

Then the uncertainty of mass flow rate, useful heat, and thermal efficiency will be;

$$\delta\dot{m} / \dot{m} = [(\delta V_{av} / V_{av})^2 + (\delta T / T)^2 + (\delta P / P)^2 \cdots (6)$$

And

$$\delta Q_u / Q_u = [(\delta\dot{m} / \dot{m})^2 + (\delta(T_o - T_{in}) / (T_o - T_{in})^2]^{1/2} \cdots (7)$$

And

$$\delta\eta / \eta = [(\delta\dot{m} / \dot{m})^2 + (\delta(T_o - T_{in}) / (T_o - T_{in})^2 + (\delta I_T / I_T)^2]^{1/2} \cdots (8)$$

2.1 Test Procedure:

The test may be summarized to:

1. Initially choose a type of porous material and then put it in the drawer which installed in the lower pass of the double passage solar heaters.
2. The blower is provided with electrical power.
3. Read the radiation intensity, after 20 minutes or more reaching to the steady state condition, at different points on the collector and take the average.
4. Change the intensity of radiation by dimming it until reaching the desired heat flux.
5. Reaching to the steady state condition, which takes one hour or more from the start of operation depending on type of porous media.
6. Adjusting the air velocity to five values using the gate.
7. Reading the values of temperatures by data logger.
8. In each value of air velocity, the pressure drop along the duct is read using a digital manometer.
9. All steps are repeated for different values of heat flux.

Everything mentioned above is repeated for each type of porous media.

3. Theory

Useful energy is,

$$Q_u = m C_P (T_{out} - T_n) \cdots (9)$$

The thermal efficiencies of the solar air heaters calculated as:

$$\eta_{th} = \frac{Q_u}{I A_C} \cdots (10)$$

The double pass solar air heater with porous media has a physical model as shown in Figure 5. The dimensions of the collector are (125×30×11) cm. Fluid (air) at ambient temperature goes through the upper channel at T_{in} and leaves from bottom channel with outlet temperature T_{out}. To simulate and build an algebraic equations of the differential governing equations using stainless-steel balls as porous material, the following assumptions were used:

1- Steady state and incompressible flow.
2- 3- d simulation.
3- The flow is turbulent.
4- Properties are assumed at average temperature.
5- The natural convection is ignored.

The solution was performed using FORTRAN 90 software with two values of porosities 62 and 33.5% (stainless steel balls as porous media). The build CFD program was used to calculate by finite volume parameters (U, V, W, T, k and ε) [41]:

$$\frac{\partial}{\partial x}(\rho U \phi) + \frac{\partial}{\partial y}(\rho V \phi) + \frac{\partial}{\partial z}(\rho W \phi) = \frac{\partial}{\partial x}(\Gamma \phi \frac{\partial \phi}{\partial x}) + \frac{\partial}{\partial y}(\Gamma \phi \frac{\partial \phi}{\partial y}) + \frac{\partial}{\partial z}(\Gamma \phi \frac{\partial \phi}{\partial z}) + S_\phi \cdots (11)$$

The left terms represents convection and the right terms represent diffusion and source terms.

The term which represents source is explained Table 1.

The empirical constants are shown in Table 2.

The numerical study includes the stainless steel balls at two porosities 33.5 and 62%. The balls arranged in symmetrical positions as shown in Figure 6. The porosity can be defined as a measure of the spaces and is a percentage of the volume of voids above the total volume. In the program the porous media location has been determined by dividing the device into a number of nodes towards X, Y and Z, then calculated the nodes occupied by porous media. At first row 50% of nodes are solid and other nodes are voids in order to get porosity equal to 50% and at the second row, the same thing happen as the first row, but it is in opposite locations and etc. Porosity 67% can be getting by make 3/4 of nodes solid and the others are voids meanwhile made 1/3 of nodes solid getting porosity equal to 33%. The velocity was zero at the nodes that solid.

- Initial conditions

Initially, $T_{amb} = 31.5\ ^{o}C$,

$U = V = W = 0$, at the place that occupied by porous media

- Conditions of the boundary

a) Velocities at all solid walls = 0.

b) At the inlet upper channel of the collector, the velocity of the stream have positive value and the velocity of air in the lower channel have negative value. Figure 7 illustrates the conditions of the boundary.

At inlet:

$$\left.\begin{cases} At, x = 0 \\ H_{down} \subset y \subset H_{up} \\ 0 \subset z \subset W \end{cases}\right\}, T = T_{in}, \quad U = U_{in}$$

For turbulence parameters:

$$k_{in} = C_k u_{in}^2$$

$$\varepsilon_{in} = C_\mu k_{in}^{3/2} / (0.5 D_h C_\varepsilon)$$

Where, $C_k = 0.003\ and\ C_\varepsilon = 0.03$).

c) At exit,

Normal gradients was used to be zero:

$$\left.\begin{cases} At \quad x = 0 \\ 0 \subset y \subset H_{down} \\ 0 \subset z \subset W \end{cases}\right\}, \quad \frac{\partial \phi}{\partial x} = 0$$

Where;

ϕ is represents $U, V, W, T, k\ and\ \varepsilon$.

The air enters the upper channel of the device at a temperature equal to the air temperature, passes through the upper passage and gains heat through the absorber plate and the radiation falling on the device, then it turns around to pass through the lower channel to pour additional heat from the absorber and porous materials, noting that the back plate is insulated.

4-Results and Discussion

Heat transfer area is increased and total heat losses are reduced with two passes collector with permeable materials. The work of the suggested counter flow solar collector with and without porous media was performed. Parameters, mass flow rate, porosity, intensity of irradiation and conductivity were tested in two parts:

Experimental part

Relationship between porosity and diameter is the opposite relationship as shown in Figure 8.

Figures 9 and 10 explain the impact of mass flow rate on the difference of temperature at various simulator radiations with and without porous material. The difference of temperature increases with decreasing fluid rate and also with porosity materials (stainless-steel and glass balls) was higher than without porosity material. Conductivity of porosity material shows an effective part of transfer of heat that led to enhance the collector efficiencies. Highest temperature difference reached 23.3 °C with stainless-steel balls and reached 19.1 °C with glass balls at 0.01773 kg/s. Temperature difference also increases as porosity decreases because the diameter of porous media increases as cleared in Figure 11.

Figures 12 and 13 show the impact of mass flow rate on the efficiency. The efficiency enhances with the increasing of mass flow rate and reaches maximum value then decreases. Putting porous material in the lower passage will increase the heat transfer and as a result, the thermal efficiency increases.

Figure 14 describes the impact of mass flow rate on efficiency with various porosities of glass and stainless-steel balls. The reduction in porosity also decreases the flow channeling, i.e. increases the tortuousness of the air flowing through the packed passage resulting in improving the efficiency. Maximum efficiency obtained when using stainless-steel balls as porous media is 85.9 percent which is higher compared with glass balls as porous media which reached 76.02 percent because of this higher thermal conductivity, which made it another heat source to heat the air. Thermal conductivity of porosity material has effective part in making the difference clear between stainless steel and glass balls as that made stainless steel balls more efficient at the same condition.

Figure 15 illustrates the effect of porous substrate thermal conductivity on the temperature difference. When it is compared between glass and stainless steel balls, thermal efficiency of stainless steel balls is higher than glass balls.

Numerical part

Figure 16 A and B demonstrates the changing of the outlet temperature with mass flow rate at various values of irradiance at two porosities.

Fluid enters at temperature 31.5 °C, and increases to the exit through porosity material. Figures 17 and 18 show isothermal contours of collector at mass flow rate of 0.0019 kg/s with 400 W/m² irradiation with two porosities 62 and 33.5% respectively.

The temperature increases in the flow direction. The existing of porosity materials in the bottom passage resulted in increasing temperatures and the effect of porous material concentrations is evident in the case of comparison between 33.5 and 62%. The output temperature with porosity 33.5% is higher as compared with 62%. This resulting obstruction of the air path and its stay in the lower pass for the longest period possible.

The flow field in 2D at 0.01063 kg/s (mass flow rate) at porosity equals 62%. It is clear that the velocity decreases and reaches zero at the walls, while it reaches max values in center. It is noted that there's no velocity in the place that occupied by porous media.

5. Validation of the numerical results

Figure 19 demonstrates the validation of the numerical results by comparing the temperatures of exit with specific mass flow rate at two porosities. These figures showed a good agreement between the experimental and numerical results for the exit air at pours media in the lower channel of the collector. The numerical results are greater than experimental values because of losses.

Due to the different practical conditions when measuring, it is difficult to find similar studies with the same conditions of work, but research [42] shows the same behavior that was discussed in the results of this work as shown in Figure 20. It obvious that the thermal efficiency for present work was 69 %, while at the research reached 50.36%.

6-Conclusions

The present work on porous media (glass spheres and stainless steel) packaged solar air heaters has been experimental and numerical research. There are many things that can be concluded:

Porous media in the bottom channel enhanced the performance of the solar collector. It acts as a heating source. Efficiency with porous media increased as porosity decreased. Thermal efficiency increases as the thermal conductivity of the porous media increases because this increases the heat exchange process. There is reasonable agreement between the experimental and numerical results.

References

[1] Kardgar, A. and Jafarian, A. “Numerical simulation of turbulent oscillating flow in porous media”, Scientia Iranica B 28(2), pp. 743-756, (2021). https://doi.org/10.24200/SCI.2020.52521.2788

[2] Abbas, Z., Rauf, A., Shehzad, S.A., et al. “Cattaneo-Christov heat and mass flux models on time-dependent swirling flow through oscillatory rotating disk”, Scientia Iranica B 28(3), pp. 1329-1341, (2021). https://doi.org/10.24200/SCI.2020.53248.3139

[3] Safarzadeh, S. and Rahimi, A. B., “Convective heat transfer and flow phenomena from a rotating sphere in porous media”, Scientia Iranica B 29(2), pp. 588-596, (2022). https://doi.org/10.24200/SCI.2021.53800.3422

[4] Roy, A. and Hoque, M. E. “Performance analysis of double pass solar air heater with packed bed porous media in Rajshahi”, In AIP Conference Proceedings (Vol. 1851, No. 1, p. 020010), AIP Publishing. (2017). https://doi.org/10.1016/j.solener.2010.07.007

[5] Maraba, G. “An experimental study on enhancement of heat transfer in a solar air heater collector by using porous medium”, İzmir Institute of Technology, (2012). http://hdl.handle.net/11147/3544, Master Thesis.

[6] Othman, M. Y. H., Sopian, K., Yatim, B., et al. “Development of advanced solar assisted drying systems”, Renewable Energy, 31(5), pp. 703-709. (2006). https://doi.org/10.1016/j.renene.2005.09.004

[7] Stanley S.G, Anbarasan, V.K., and Murugavel, K.K. “Performances of packed bed double pass solar air heater with different inclinations and transverse wire mesh with different intervals”, Thermal Science, 20, pp. 85-85. (2014). https://doi.org/10.2298/TSCI131015085S

[8] El-Khawajah, M. F, Aldabbagh L. B. Y., and Egelioglu F., “The effect of using transverse fins on a double pass flow solar air heater using wire mesh as an absorber”, Solar Energy, 85(7), pp. 1479-1487, (2011). https://doi.org/10.1016/j.solener.2011.04.004

[9] Singh, S. and Dhiman, P. “A numerical evaluation of thermal performance of double flow packed bed solar air heaters”, International Journal of Renewable Energy Technology, 4(3), pp. 242-264, (2013). https://doi.org/10.1504/IJRET.2013.054759

[10] Dhiman, P., Thakur, N. S., and Chauhan, S. R. “Thermal and thermohydraulic performance of counter and parallel flow packed bed solar air heaters”, Renewable Energy, 46, pp. 259-268, (2012). https://doi.org/10.1016/j.renene.2012.03.032

[11] El-Sebaii, A. A., Aboul-Enein, S., Ramadan, M. R. I., et al. “Year round performance of double pass solar air heater with packed bed”, Energy Conversion and Management, 48(3), pp. 990-1003, (2007). https://doi.org/10.1016/j.enconman.2006.08.010

[12] Singh, S. and Dhiman, P. “Double duct packed bed solar air heater under combined single and recyclic double air pass”, Journal of Solar Energy Engineering, 138(1), (2016). https://doi.org/10.1115/1.4032142

[13] Ozgen, F., Esen, M. and Esen, H. “Experimental investigation of thermal performance of a double-flow solar air heater having Aluminium cans”, Renewable Energy, 34(11), pp. 2391-2398, (2009). https://doi.org/10.1016/j.renene.2009.03.029

[14] Ho, C. D., Lin, C. S., Chuang, Y. C., et al. “Performance improvement of wire mesh packed double-pass solar air heaters with external recycle”, Renewable energy, 57, pp. 479-489, (2013). https://doi.org/10.1016/j.renene.2013.02.005

[15] El-Sebaii, A. A., Aboul-Enein, S., Ramadan, M. R. I., et al. “Thermal performance investigation of double pass-finned plate solar air heater”, Applied Energy, 88(5), pp. 1727-1739, (2011). https://doi.org/10.1016/j.apenergy.2010.11.017

[16] Ansari, M. and Bazargan, M. “Optimization of flat plate solar air heaters with ribbed surfaces”, Applied Thermal Engineering, 136, pp. 356-363, (2018). https://doi.org/10.1016/j.applthermaleng.2018.02.099

[17] Mohammadi, K. and Sabzpooshani, M. “Appraising the performance of a baffled solar air heater with external recycle”, Energy Conversion and Management, 88, pp. 239-250, (2014). https://doi.org/10.1016/j.enconman.2014.08.009

[18] Alam, T. and Kim, M. H.”Performance improvement of double-pass solar air heater–A state of art of review”, Renewable and Sustainable Energy Reviews, 79, pp. 779-793, (2017). https://doi.org/10.1016/j.rser.2017.05.087

[19] Saha, S. N. “Thermal Performance of Single and Double Exposure Solar Air Heaters”, Available at SSRN, pp. 3567422. (2020). https://doi.org/10.2139/ssrn.3567422

[20] Hirasawa, S., Tsubota, R., Kawanami, T et al. “Reduction of heat loss from solar thermal collector by diminishing natural convection with high-porosity porous medium”, Solar Energy, 97, pp. 305-313, (2013). https://doi.org/10.1016/j.solener.2013.08.035

[21] Meria, F. H., Algburi, S., and Omer, K. Ahmed, "Impact of porous media on PV/thermal system performance", A short review, Energy report, 11, pp. 1803-1819, (2024).
https://doi.org/10.1016/j.egyr.2024.01.046

[22] Dhiman, P., Thakur, N. S. and Chauhan, S. R. "Thermal and thermohydraulic performance of counter and parallel flow packed bed solar air heaters", Renewable Energy, 46, pp. 259-268 (2012).
https://doi.org/10.1016/j.renene.2012.03.032

[23] Gupta, B., Manikpuri, G. P., Waiker, J. K., et al. "Experimental investigation of double pass solar air heater using different type of porous media", Int J Curr Eng Tech, 3(5), pp. 2006-2009, (2013).
http://inpressco.com/category/ijcet

[24] Jouybari, N. F. and Lundström, T. S. "Performance improvement of a solar air heater by covering the absorber plate with a thin porous material", Energy, 190, (2020).
https://doi.org/10.1016/j.energy.2019.116437

[25] Kareem, M. W., Gilani, S. I., Habib, K., et al. "Performance analysis of a multi-pass solar thermal collector system under transient state assisted by porous media", Solar Energy, 158, pp.782-791, (2017).
https://doi.org/10.1016/j.solener.2017.10.016

[26] Singh, S. "Experimental and numerical investigations of a single and double pass porous serpentine wavy wire mesh packed bed solar air heater", Renewable Energy, 145, pp. 1361-1387, (2020).
https://doi.org/10.1016/j.renene.2019.06.137

[27] Singh, S., Dhruw, L. and Chander, S. "Experimental investigation of a double pass converging finned wire mesh packed bed solar air heater", Journal of Energy Storage, 21, pp. 713-723, (2019).
https://doi.org/10.1016/j.est.2019.01.003

[28] Kansara, R., Pathak, M., and Patel V.K. "Performance assessment of flat-plate solar collector with internal fins and porous media through an integrated approach of CFD and experimentation", International Journa of thermal Sciences, 165, (2021).
https://doi.org/10.1016/j.ijthermalsci.2021.106932

[29] Ahmed, O. K. and Mohammed, Z. A. "Influence of porous media on the performance of hybrid PV/Thermal collector", Renewable Energy, 112, pp. 378-387, (2017).
https://doi.org/10.1016/j.renene.2017.05.061

[30] Salih, S.M., Jalil, J.M., and Najim, S.E., "Experimental and numerical analysis of double-pass solar air heater utilizing multiple capsules PCM", Renewable Energy, 143, pp. 1053–1066, (2019).
https://doi.org/10.1016/j.renene.2019.05.050

[31] Salih, S.M., Jalil, J.M., and Najim, S.E., "Comparative study of novel solar air heater with and without latent energy storage", Journal of Energy Storage, 32, (2020). https://doi.org/10.1016/j.est.2020.101751

[32] Dawood, N.I., Jalil, J.M., and Ahmed, M.K., "Investigation of a novel window solar air collector with 7-moveable absorber plates, Energy, 257, (2022). https://doi.org/10.1016/j.energy.2022.124829

[33] Fu, Y., Xia, Y., Lin, X., et al. "A novel structure design and numerical analysis of porous media-assisted enhanced thermal performance of flat-plate solar collector", Thermal Science and Engineering Progress 40 (2023). https://doi.org/10.1016/j.tsep.2023.101777

[34] Siavashi, M., Bozorg, M. V., and Toosi, M. H., "A numerical analysis of the effects of nanofluid and porous media utilization on the performance of parabolic trough solar collectors", Sustainable Energy Technologies and Assessments 45, (2021). https://doi.org/10.1016/j.seta.2021.101179

[35] Xia, Y., Lin, X., Shu, Y., et al., "Enhanced thermal performance of a flat-plate solar collector inserted with porous media: A numerical simulation study", Thermal Science and Engineering Progress 44 (2023). https://doi.org/10.1016/j.tsep.2023.102063

[36] Mustafa, J., Alqaed, S., and Sharifpur, M., "Enhancing the energy and exergy performance of a photovoltaic thermal system with ∇-shape collector using porous metal foam", Journal of Cleaner Production 368 133121 (2022). https://doi.org/10.1016/j.jclepro.2022.133121

[37] Helmi, N., Nazari, A., Bezaatpour, M., et al. "Investigation of energy storage in parabolic rotary trough solar collectors using various porous fins with magnetic nanoparticles", Energy for Sustainable Development 70, pp. 194–204 (2022). https://doi.org/10.1016/j.esd.2022.07.009

[38] Khelifa, A., Kabeel, A. E., Attia, M. E, et al. "Numerical analysis of the heat transfer and fluid flow of a novel water-based hybrid photovoltaic-thermal solar collector integrated with flax fibers as natural porous materials", Renewable Energy 217, (2023). https://doi.org/10.1016/j.renene.2023.119245

[39] Bozorgi, M., Ghasemi, K., Mohaghegh, M. R., et al. "Optimization of silver/water-based porous wavy direct absorption solar collector", Renewable Energy 202 pp. 1387–1401, (2023). https://doi.org/10.1016/j.renene.2022.11.065

[40] Darbari, B., Derikvand, M., and Shabani, B.," Thermal performance improvement of a LS-2 parabolic trough solar collector using porous disks", Applied Thermal Engineering 228, (2023).

https://doi.org/10.1016/j.applthermaleng.2023.120546

[41] Versteeg, H. K. and Malalasekera, W., "An introduction to computational fluid dynamics", the finite volume method: Pearson education, 2007, Book.

[42] Yousef, B. A. A. and Adam, N. M. “Performance analysis for flat plate collector with and without porous media”, Journal of Energy in Southern Africa, 19(4), pp. 32-42, (2008).
http://dx.doi.org/10.17159/2413-3051/2008/v19i4a3336

Caption of Tables

Caption of Figures

- Figure 17. Isothermal contours of collector at mass flow rate 0.0019 kg/s and at irradiance 400 W/m² and porosity 62%.

- Figure 18. Isothermal contours of collector at mass airflow of 0.0019 kg/s, irradiance 400 W /m² and porosity 33%.

- Figure 19.Changing of experimental and numerical outlet temperature with mass flow rate (A) φ=62% (B) φ=33.5%.

- Figure 20. Changing of the efficiency with mass flow rate for present study and Ref [42] study (stainless steel wire mesh) at irradiance 600 W/m^2 and porosity 96%.

Tables

Nomenclature	
A_C	Collector area, m^2
C_P	Specific heat, kJ/kg K
Q_u	Gain of heat (useful), W
$\dot{m}$	Mass Flow rate, kg/sec
T_{out}, T_{in}	Exit and in temperatures, ^{o}C
Q	Radiation intensity, W/m^2
P	Air density, kg/m^3
U, V, W	Component of the velocities, m/sec
Γ	Coefficient of diffusion, kg/m sec
S_ϕ	Term of the source
ϕ	Variable
K	conductivity, W/m K
ε	Rate of dissipation
$C_{1\varepsilon}, C_{2\varepsilon}, C_k$	Constants
$\sigma_k, \sigma_\varepsilon$	Number of Prandtl for turbulent flow
Φ	Porosity
WOPM	Without porous media

Table 1: Details of source expression

Equation	ϕ	Γ_ϕ	S_ϕ
Continuity	1	0	0
U-momentum	U	Γ_u	$-\frac{\partial P}{\partial x}+\frac{\partial}{\partial x}(v_e\frac{\partial U}{\partial x})+\frac{\partial}{\partial y}(v_e\frac{\partial V}{\partial x})+\frac{\partial}{\partial z}(v_e\frac{\partial W}{\partial x})$
V-momentum	V	Γ_v	$-\frac{\partial P}{\partial y}+\frac{\partial}{\partial x}(v_e\frac{\partial U}{\partial y})+\frac{\partial}{\partial y}(v_e\frac{\partial V}{\partial y})+\frac{\partial}{\partial z}(v_e\frac{\partial W}{\partial y})$
W-momentum	W	Γ_w	$-\frac{\partial P}{\partial z}+\frac{\partial}{\partial x}(v_e\frac{\partial U}{\partial z})+\frac{\partial}{\partial y}(v_e\frac{\partial V}{\partial z})+\frac{\partial}{\partial z}(v_e\frac{\partial W}{\partial z})$
Temperature	T	Γ_T	0
Kinetic Energy	k	Γ_k	$G-\varepsilon$
Dissipation Rate	ε	Γ_ε	$C_{1\varepsilon}\frac{\varepsilon}{k}G-C_{2\varepsilon}\frac{\varepsilon^2}{k}$

Table 2: The constants of (k-ε) equation [28].

C_μ	$C_{1\varepsilon}$	$C_{2\varepsilon}$	σ_k	σ_ε
0.09	1.44	1.92	1.00	1.30

Figures

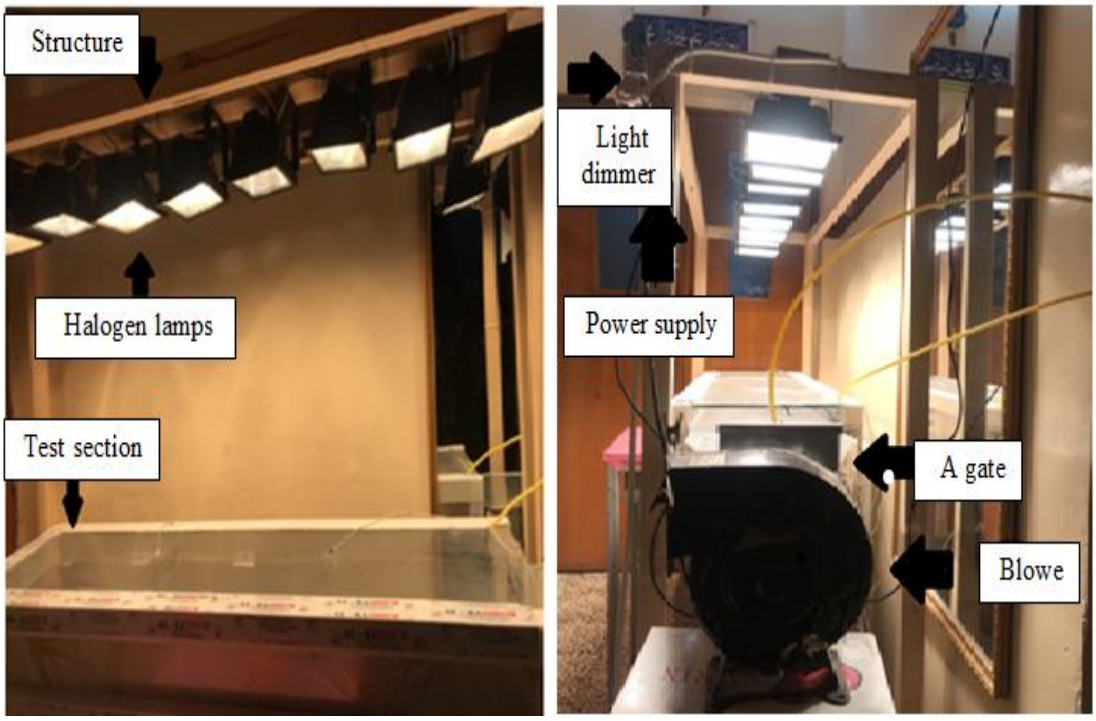

(a) **(b)**

Figure 1. Experimental equipment with two views

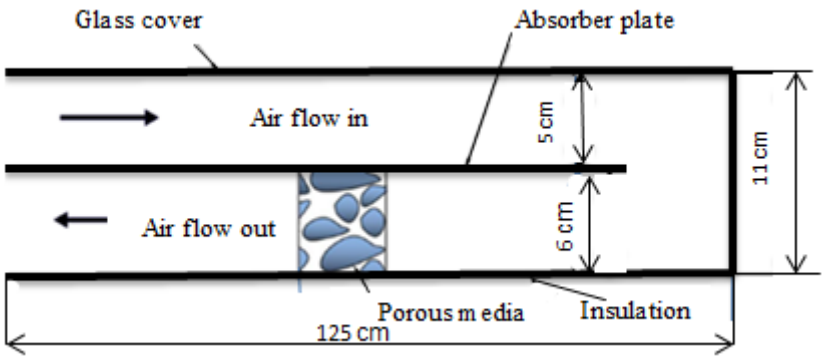

Figure 2. The schematic of double pass thermal solar collector with porous media in second channel

(A)

(B)

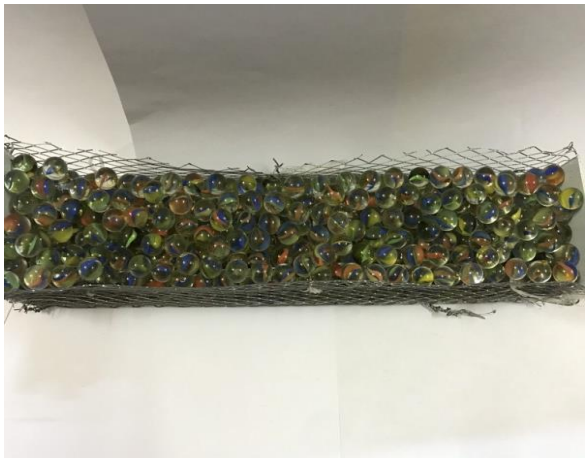

(C)

Figure 3. Glass balls (A) D=2.3 cm (B) D=1.622 cm (C) D=1.1367 cm

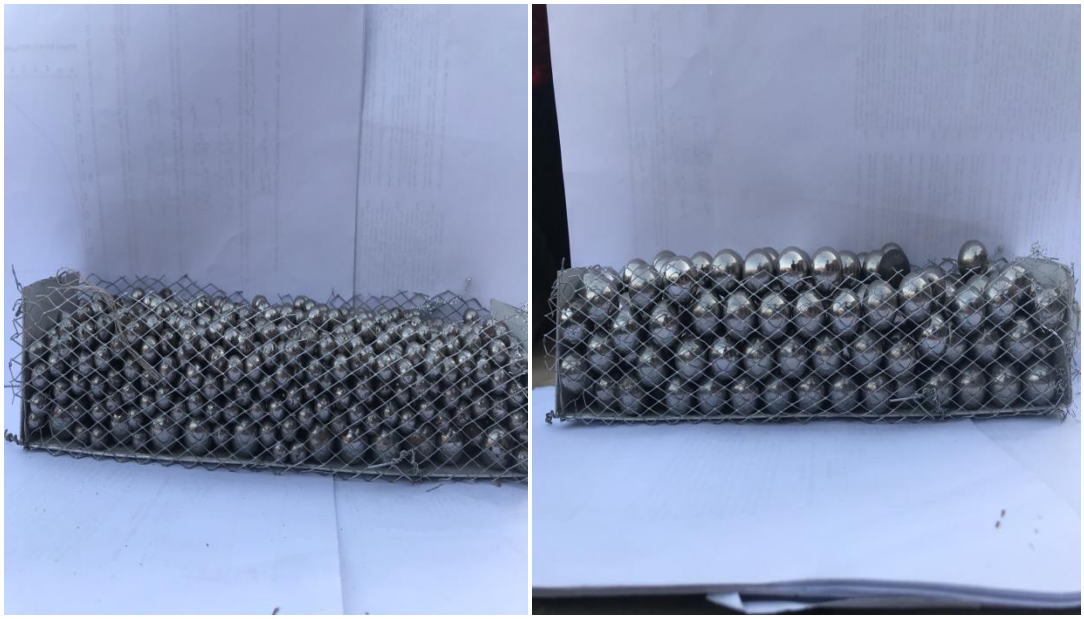

(A) (B)

Figure 4. Stainless steel balls (A) D=1.9 cm (B) D=1.137 cm

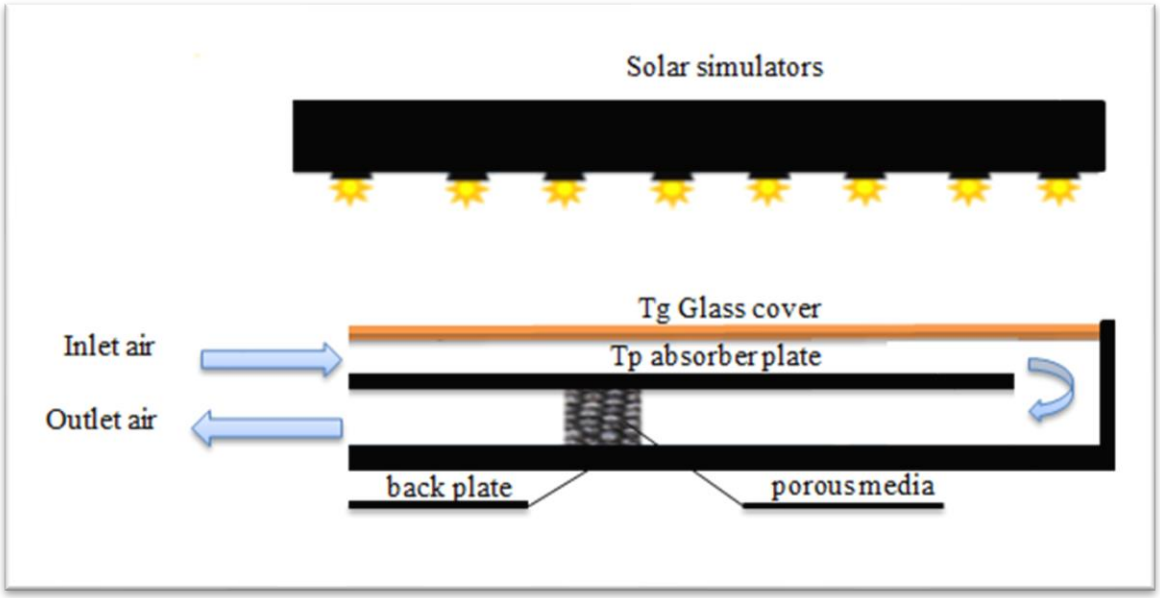

Figure 5. The solar air collector physical model

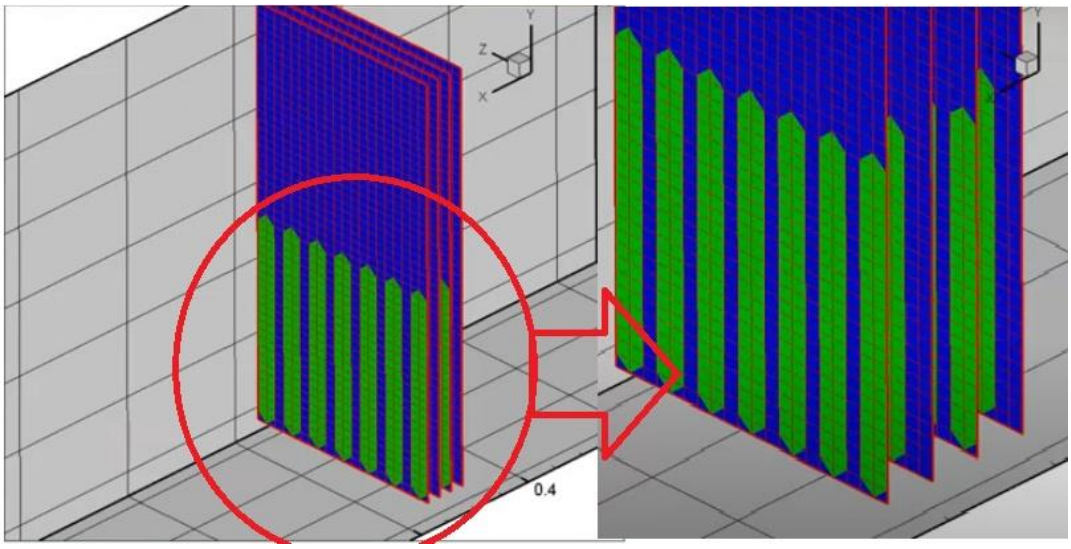

Figure 6. Arrangement of balls with symmetrical sites

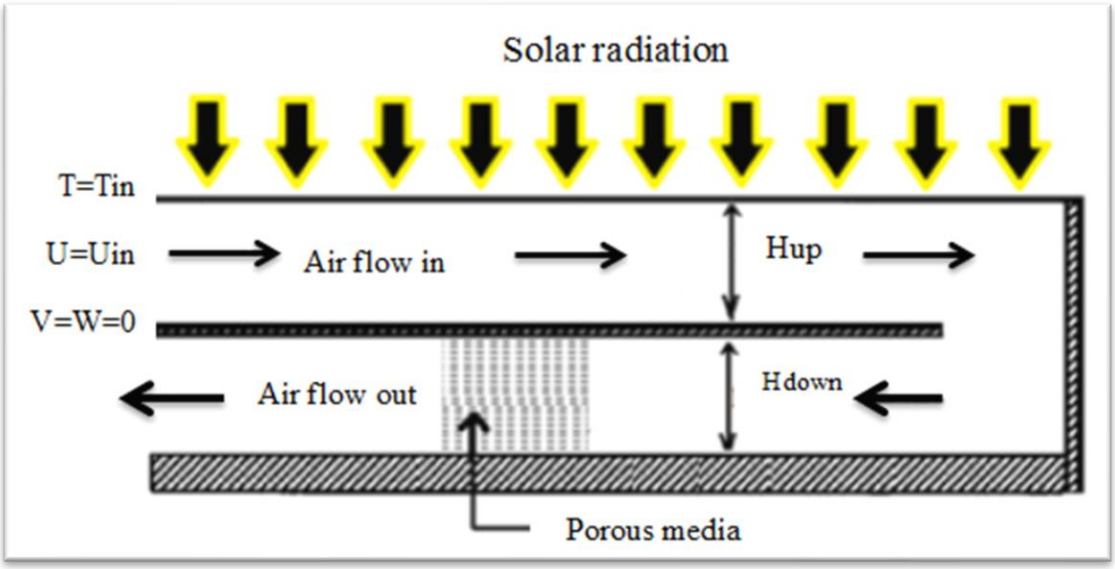

Figure 7. Boundary conditions

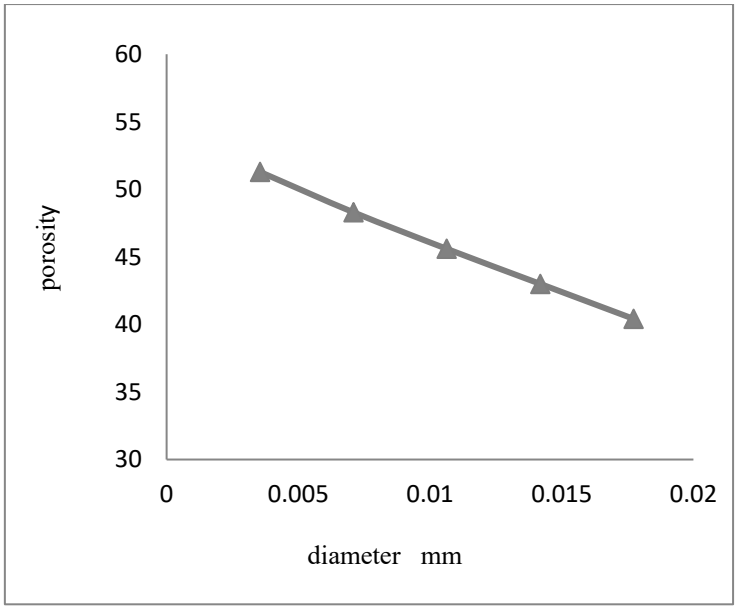

Figure 8. The effect of diameter on porosity

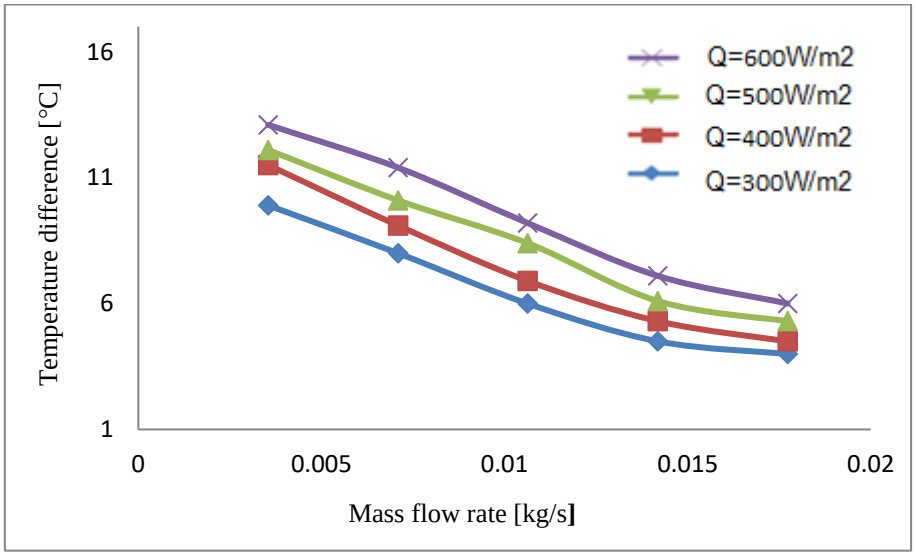

Figure 9. Variation of temperature difference with mass flow rate without porous materials at different solar irradiations W/m^2

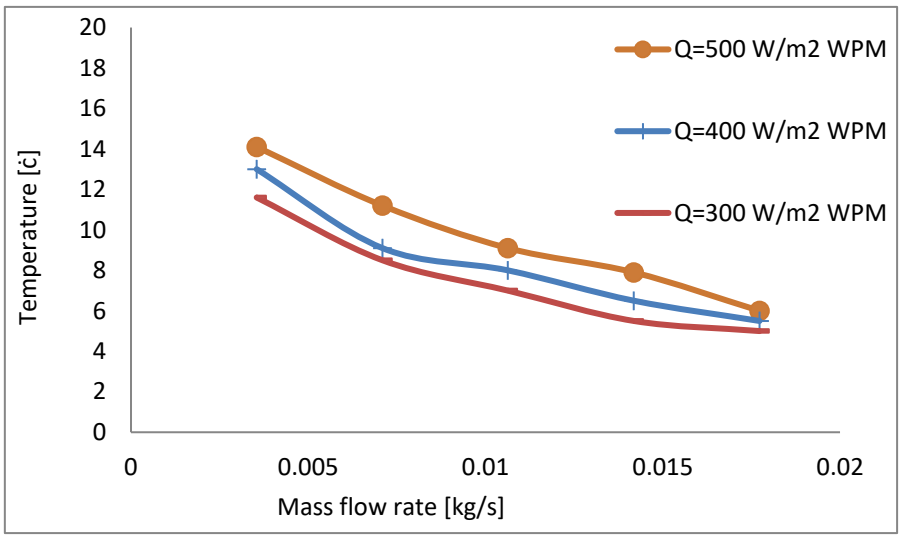

Figure 10. Impact of the difference of temperature with mass flow rate (glass balls with D=1.622 cm) at different solar irradiations W/m^2

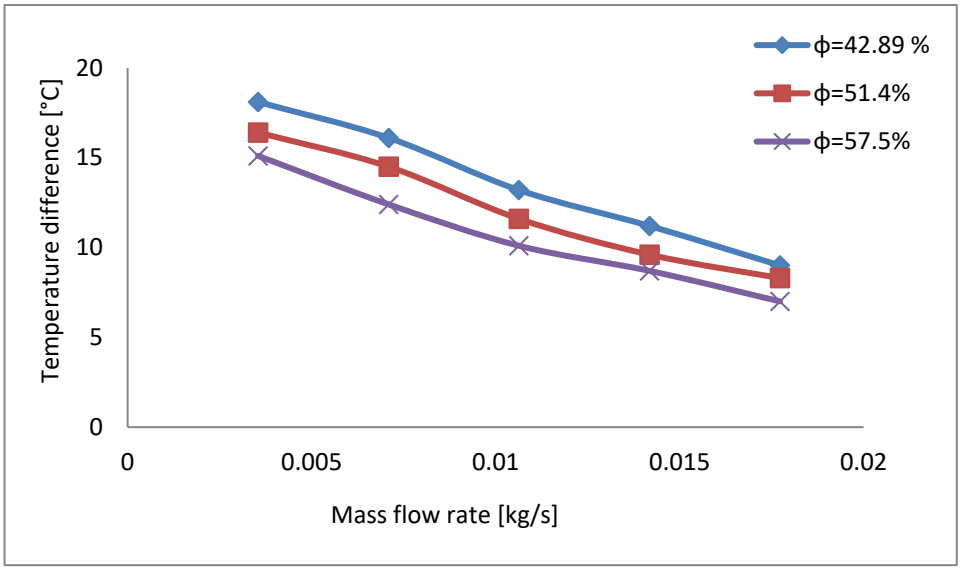

(A)

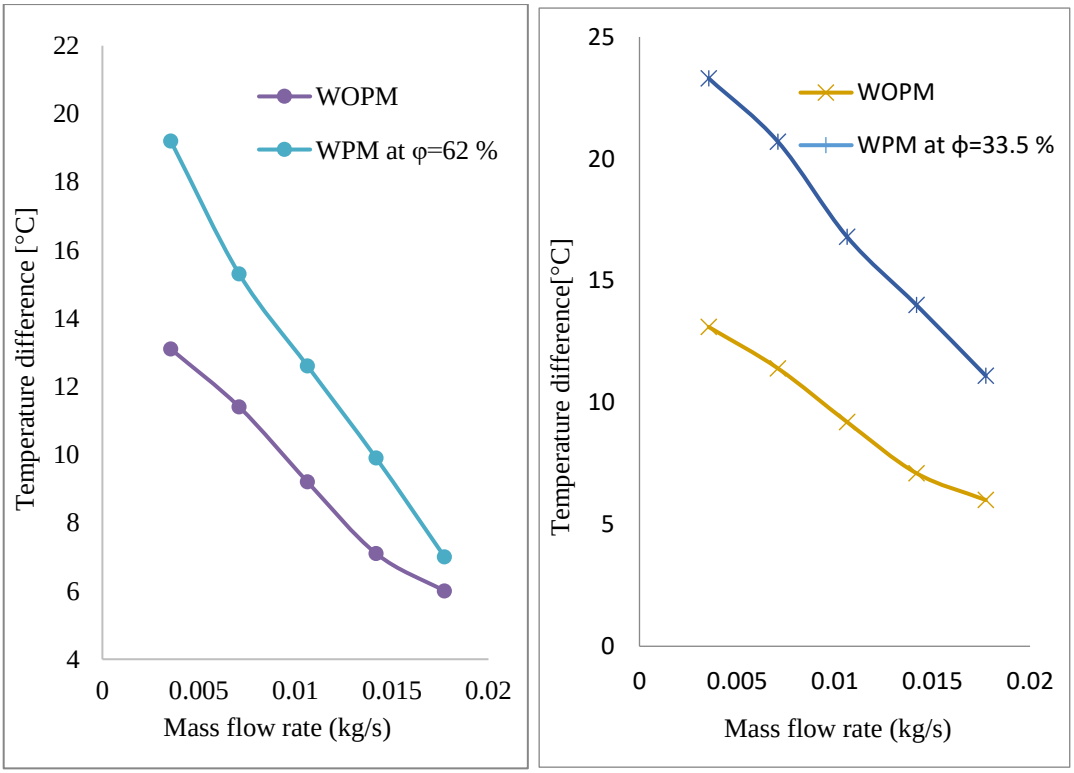

(B)

Figure 11. Variation of temperature difference with mass rate at different porosities with radiation 500 W / m^2 (A) glass balls (B) stainless balls porosity **(**62% **,** 33.5%**)**

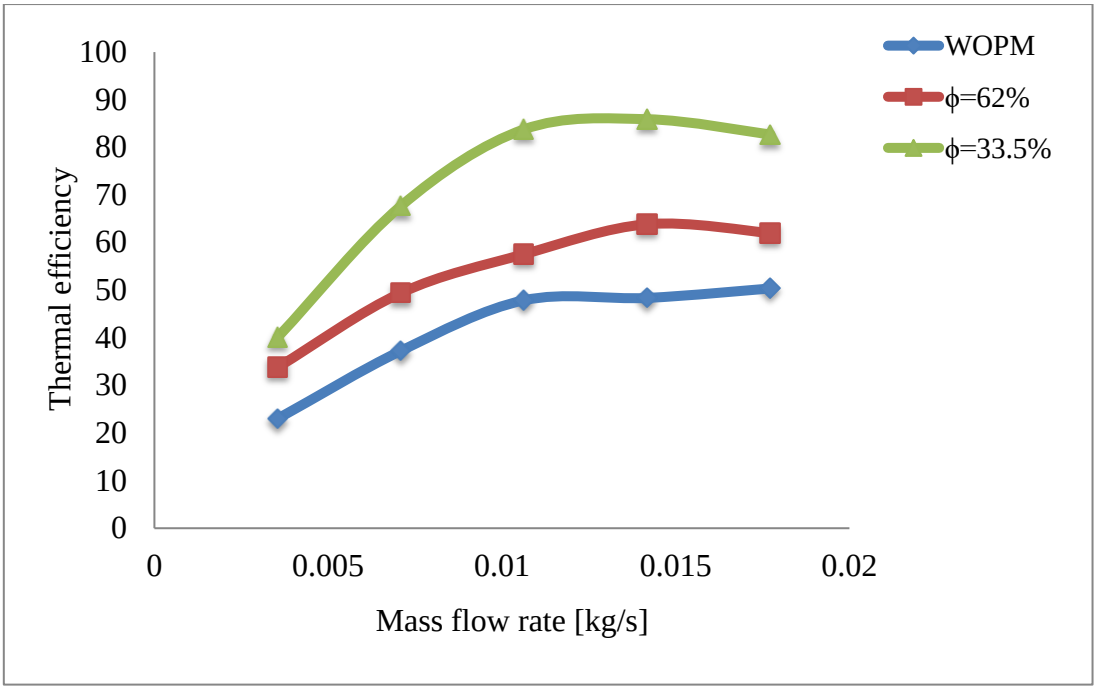

Figure 12. The impact of mass flow rate on the efficiency with and without porous media (stainless steel balls)

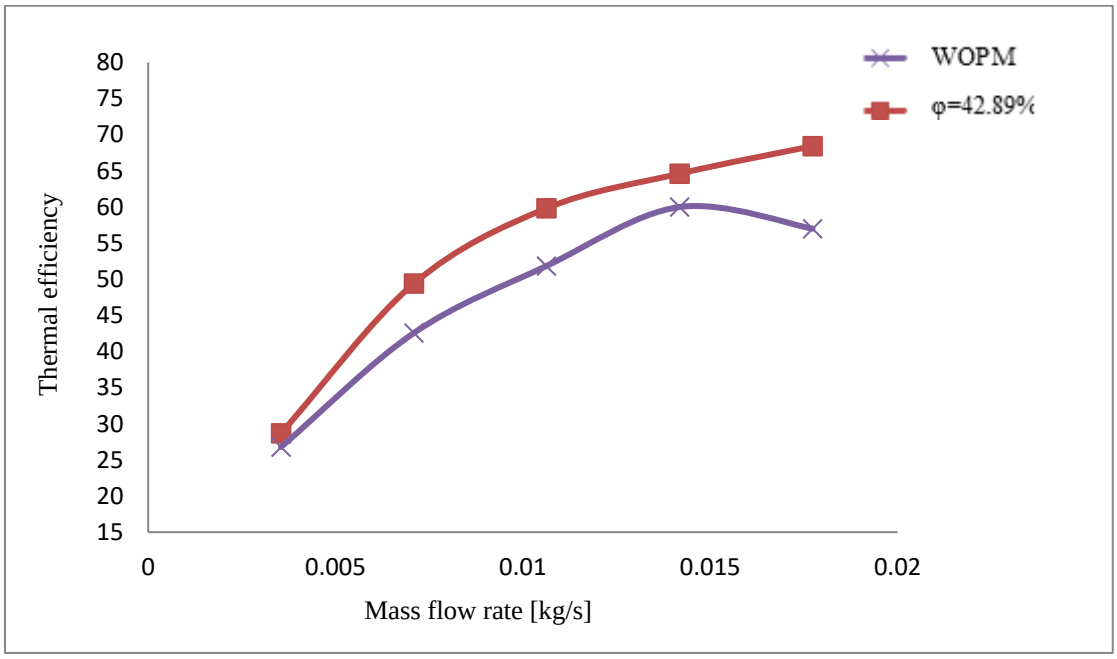

Figure 13. Changing of the thermal efficiency with and without porosty material (glass)

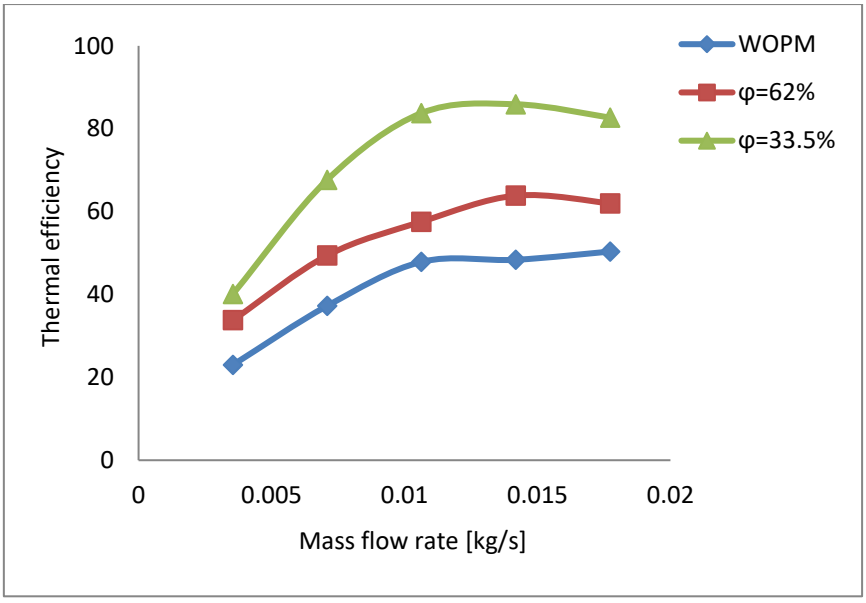

(a)

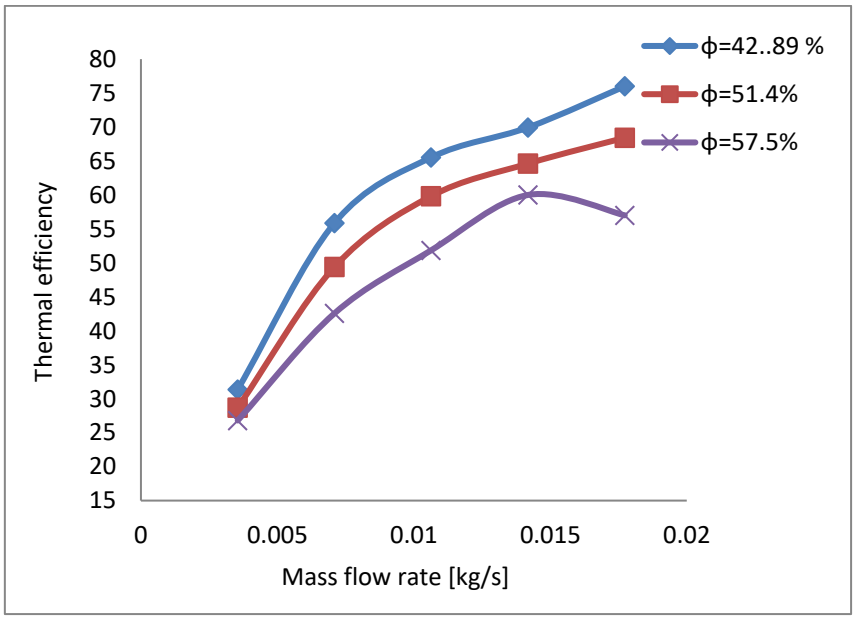

(b)

Figure 14. The impact of air rate on the efficiency at flux = 500 W/m^2 with various porosities (a) stainless-steel balls (b) glass balls

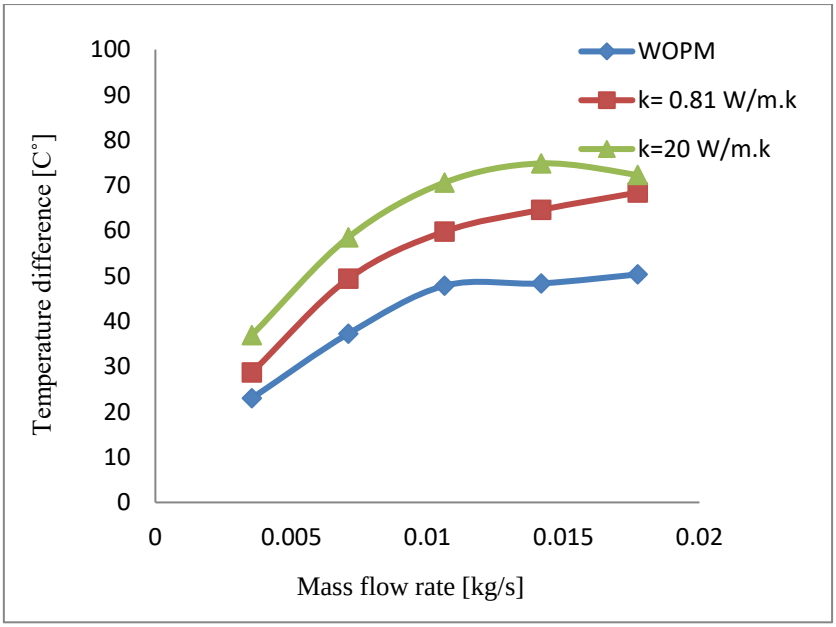

Figure 15. Variation of temperature difference with air rate for various conductivities

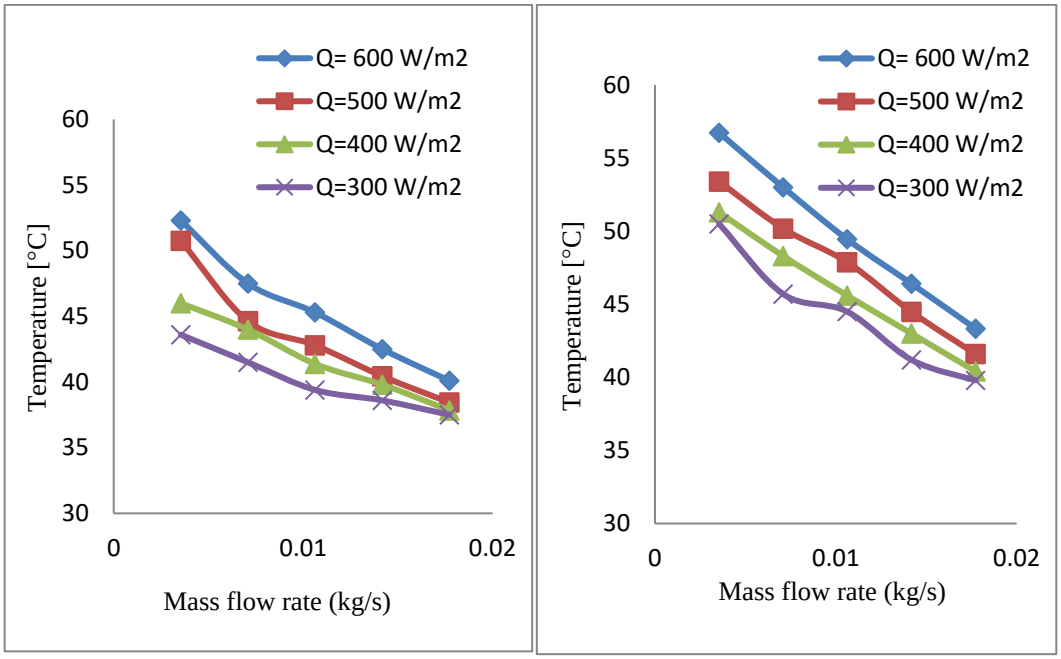

(A) (B)

Figure 16. Changing of the air temperature of air outlet with mass flow rate (different irradiances) (A) porosity = 62% (B) porosity = 33.5%, numerical results

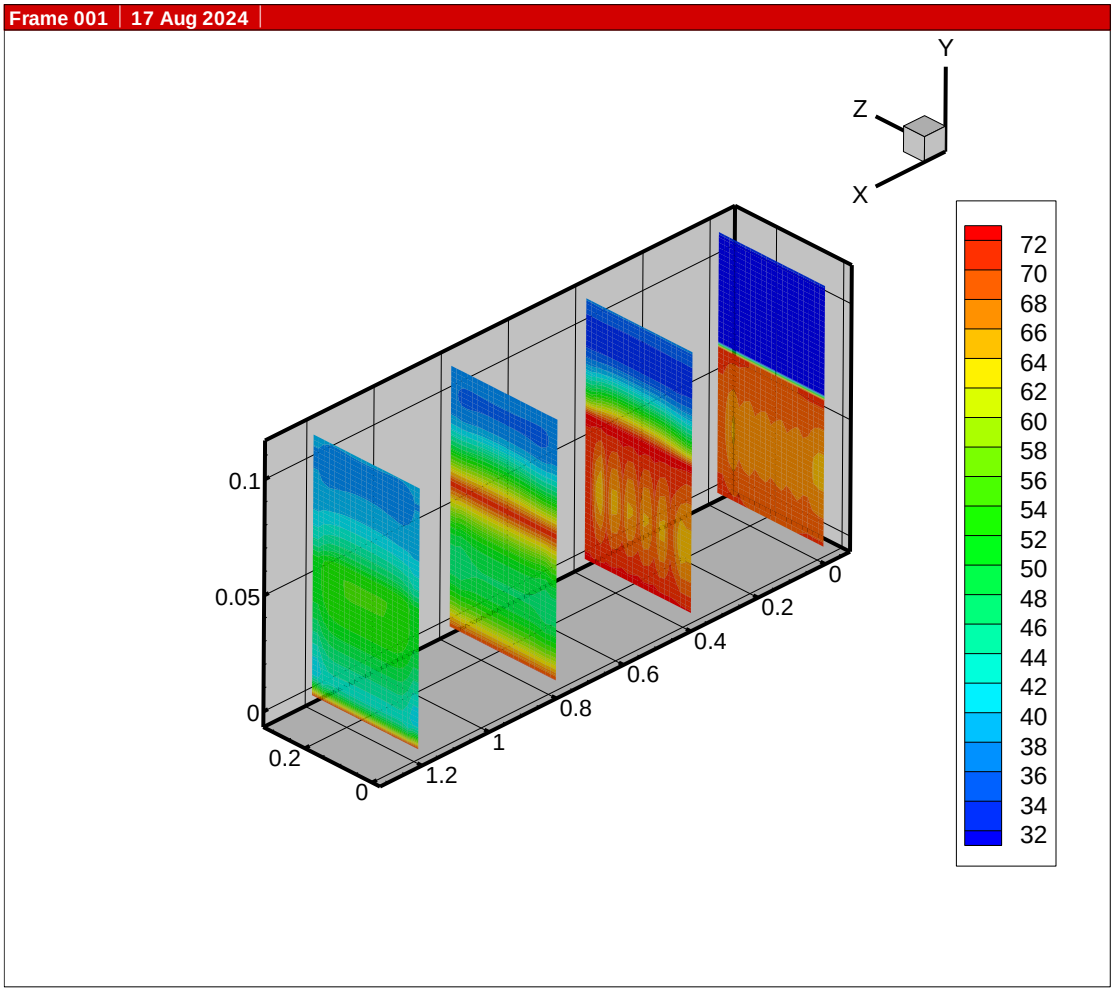

Figure 17. Isothermal contours of collector at mass flow rate 0.0019 kg/s and at irradiance 400 W/m² and porosity 62%.

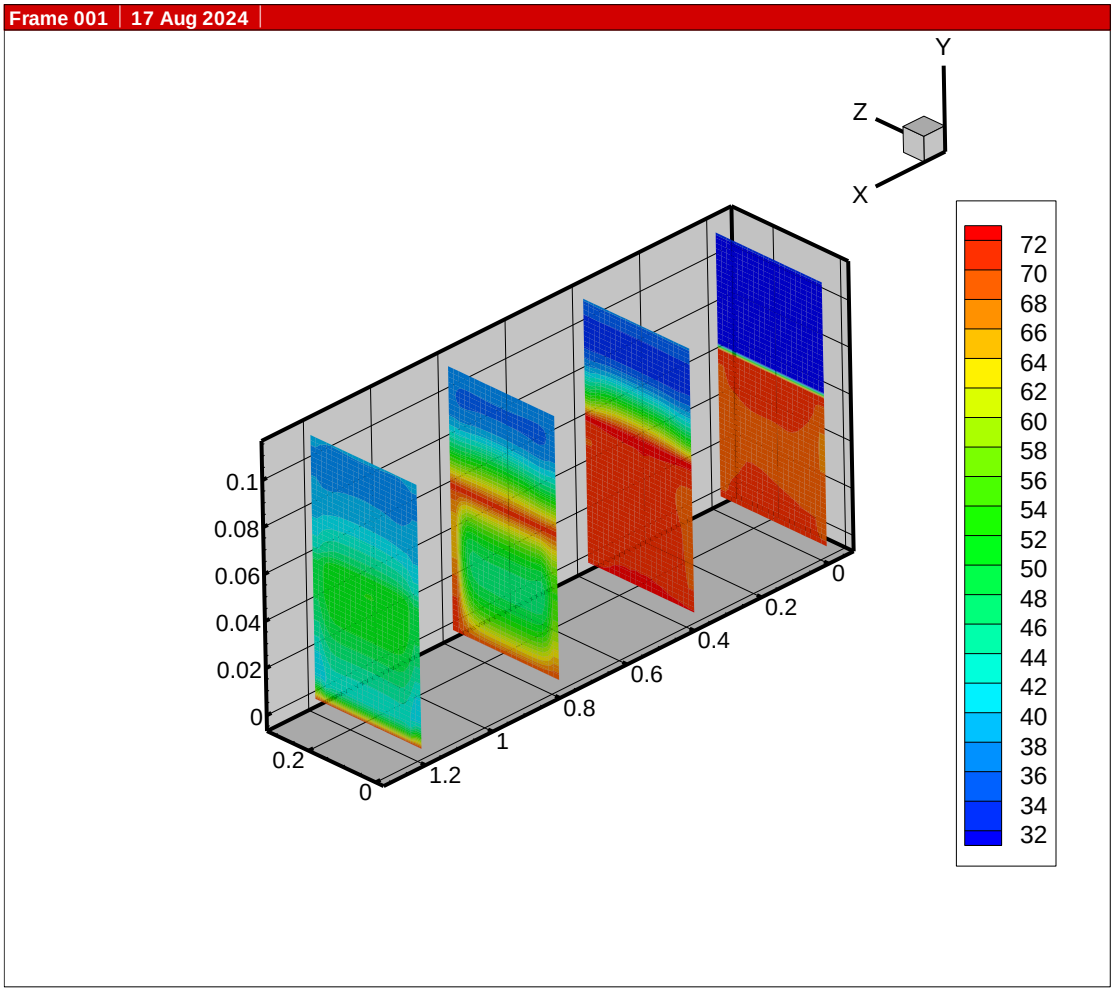

Figure 18. Isothermal contours of collector at mass airflow of 0.0019 kg/s, irradiance 400 W /m² and porosity 33%.

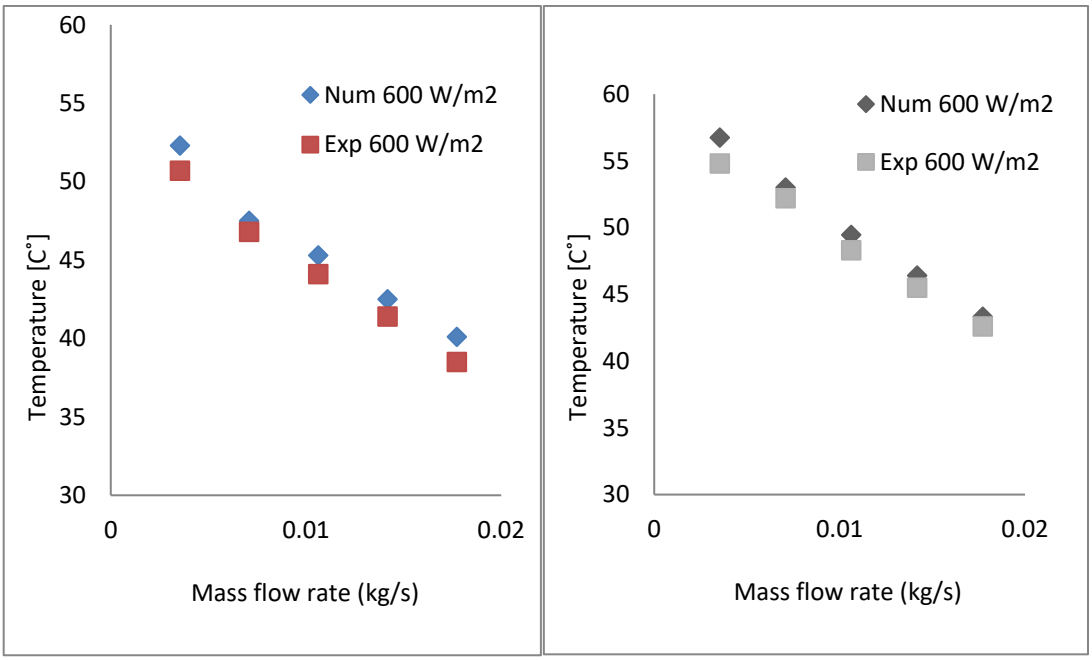

A B

Figure 19. Changing of experimental and numerical outlet temperature with mass flow rate (A) φ=62% (B) φ=33.5%

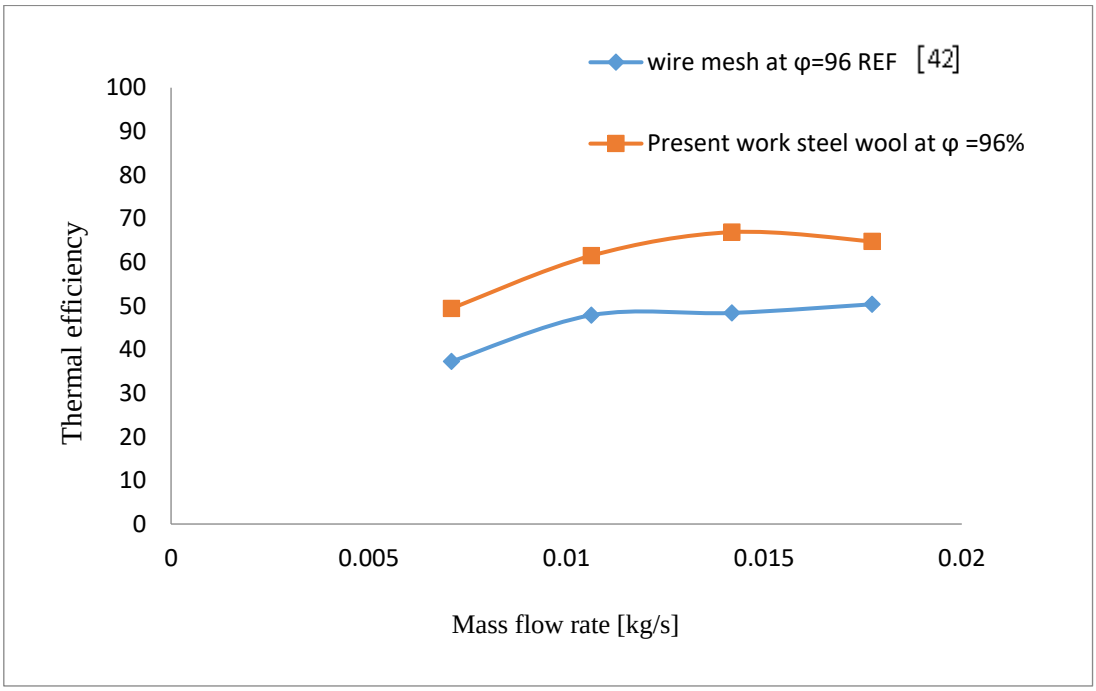

Figure 20. Changing of the efficiency with mass flow rate for present study and Ref [42] study (stainless steel wire mesh) at irradiance 600 W/m^2 and porosity 96%

Brief biographies of all authors:

Dr. Jalil was born in Basra in south Iraq. He obtained his Bachelor degrees in Mechanical Engineering from the University of Baghdad (1980) and PhD from University of Liverpool (1989). He joined the academic staff at MCE in 1989. He became a Professor in 2003 and joined Electromechnical Engineering Department in University of Technology. His research background is in the general area of computational fluid dynamics and heat transfer where he have published over 173 papers, and have supervised 92 MSc and PhD students.

Dr. Shereen was born in Basra in south Iraq. She obtained her Bachelor in Electrical Engineering from University of Basra (1985) and PhD from University of Technology (2004). She joined the Electromechanical Engineering Department in University of Technology in 1993. She became an assistant professor in 2010. Her research background is in the general area of Electrical machines where as she has published over than 20 papers, and has supervised 8 MSc students.

Shrooq was born in Baghdad. She obtained her Bachelor degrees in Electromechanical Engineering from the University of Technology (2016) and MSc from University of Technology (2020). She joined the academic staff in Private universities for two years . After that, she worked in the Ministry of Electricity in the field of energy engineering and renewable energies.